

Electron Beam-Melted, Free-Form-Fabricated Titanium Alloy Implants: Material Surface Characterization and Early Bone Response in Rabbits

Peter Thomsen,¹ Johan Malmström,¹ Lena Emanuelsson,¹ Magnus René,² Anders Snis²

¹ Department of Biomaterials, The Sahlgrenska Academy, University of Gothenburg, SE-405 30 Göteborg, Sweden

² Arcam AB, Krokslätts Fabriker 27 A, SE-431 37 Mölndal, Sweden

Received 19 September 2007; revised 4 June 2008; accepted 8 August 2008

Published online 5 November 2008 in Wiley InterScience (www.interscience.wiley.com). DOI: 10.1002/jbm.b.31250

Abstract: Titanium-6aluminum-4vanadium implants (Ti6Al4V) were prepared by free-form-fabrication (FFF) and were used either as produced or after machining and compared with wrought machined Ti6Al4V. Auger electron spectroscopy (AES), depth profiles, and interferometry were used to analyze the surface properties. The tissue response after 6-weeks in rabbit femur and tibia was evaluated using light microscopy and histomorphometry. The results revealed that the bulk chemical and mechanical properties of the reference material and the electron beam-melted (EBM) material were within the ASTM F136 specifications. The as-produced EBM Ti6Al4V implants had increased surface roughness, thicker surface oxide and, with the exception of a higher content of Fe, a similar surface chemical composition compared with machined EBM Ti6Al4V and machined, wrought Ti6Al4V implants. The two latter implants did not differ with respect to surface properties. The general tissue response was similar for all three implant types. Histomorphometry revealed a high degree of bone-to-implant contact (no statistically significant differences) for all the three implant types. The present results show that the surface properties of EBM Ti6Al4V display biological short-term behavior in bone equal to that of conventional wrought titanium alloy. The opportunity to engineer geometric properties provides new and additional benefits which justify further studies. © 2008 Wiley Periodicals, Inc. *J Biomed Mater Res Part B: Appl Biomater* 90B: 35–44, 2009

Keywords: electron beam melting; free-form-fabrication; surface properties; histomorphometry; bone; osseointegration

INTRODUCTION

Osseointegrated titanium implants have revolutionized treatment when it comes to the reconstruction and rehabilitation of patients.¹ Implants are surgically inserted in the bone according to strict protocols for gentle, atraumatic surgery, allowing the peri-implant tissue to undergo the phases of inflammation, regeneration, and remodeling. Under normal circumstances, this leads to the formation of new, mineralized bone adjacent to and in contact with the material surface, and the biomechanically acceptable anchorage of the implant in bone, able to withstand the load imposed by chewing, for example.²

The first generation of oral titanium implants was usually produced by machining, providing a threaded or

cylindrical macrodesign, with a surface chemistry and topography dependent on the type of material, conditions during machining, and any possible postmanufacturing steps, such as cleaning and sterilization. The second generation of these implants is often based on a combination of machining and subsequent surface treatment, for example, blasting with particles, etching, and passivation/oxidation regimens, usually providing a different microstructure and microtopography.

Clinically, patients with nonoptimal local tissue and healing properties pose a great challenge. In the same way, larger defects and aesthetic considerations warrant additional implant and surgical solutions.^{3–5} Interest is currently focusing primarily on optimizing the material properties, surgery, and monitoring for the immediate and/or early loading of implants.^{6–10} Taken together, the clinical needs provide a strong incentive for the development of new, customized implants,^{11,12} preferably allowing tissue on- and in-growth beyond the potential offered by the current first generations of implants. In addition, the combination of these third-generation implants and the delivery of biological molecules and cells is a plausible route.¹³

Correspondence to: P. Thomsen (e-mail: peter.thomsen@biomaterials.gu.se)

Contract grant sponsor: The Swedish Research Council; Contract grant number: grant 09495

Contract grant sponsor: Vinnova Forska Väx program

© 2008 Wiley Periodicals, Inc.

Traditional machining or processing techniques are not able to create these features. The advantages are at least twofold. Firstly, new research tools are provided, allowing a variety of complex geometries to be created in a reproducible manner. One obvious strong research orientation focuses on the preparation of scaffolds for tissue engineering purposes. A recent example is a series of studies of the biological effects of different ceramic materials with identical or varied 3D macro- and microporous interconnectivity.¹⁴ Secondly, individual computer-aided design (CAD) and free-form-fabrication (FFF) implants for specific bone sites (usually larger defects) in patients can now be tailored and manufactured, providing a much greater opportunity to achieve improved biological and aesthetic results. Initially, the selection of material is likely to be largely influenced by the mechanical requirements of the local tissue.

The bulk and surface properties of an implant material are influenced by the manufacturing process. Further, the subsequent treatments steps, including cleaning and sterilization, affect the composition of the outermost surface layers in contact with biological components. It is therefore of the utmost importance that the material bulk and surface properties of FFF-manufactured implants are fully characterized and that these properties are evaluated in a biological environment before clinical introduction. A recent literature survey¹⁴ indicates that very few experimental and clinical studies using FFF-produced implants have been performed. In fact, to the authors' knowledge, there are no studies in which the surface properties of FFF-produced metal and its biological properties have been described and compared with conventionally manufactured material.

The purpose of this study was, first, to determine the surface properties of titanium-6aluminum-4vanadium implants manufactured by electron beam melting [electron beam-melted (EBM); Arcam, Sweden]¹⁵⁻¹⁷ before and after machining and, second, to evaluate the early bone response (osseointegration) in rabbits. A titanium-6aluminum-4vanadium implant prepared by machining from a wrought rod (commercial supplier) was used as a control.

MATERIALS AND METHODS

Material

Forty-eight circular implants with a diameter of 3.75 mm and a length of 4 mm were prepared by:

- Machining conventionally produced bulk Ti6Al4V material.
- Machining FFF bulk Arcam Ti6Al4V extra low interstitial (ELI) material.
- Using net-shaped FFF Arcam Ti6Al4V ELI material.

All the implants were machined (Wennbergs Finmek AB, Gunnilse, Sweden) and subsequently blasted with the same Ti6Al4V ELI powder as that used in FFF production.

There were 16-implants in each of the groups A, B, and C. In Figure 1, scanning electron micrographs of three samples, one from each group, are shown.

Free-Form-Fabrication

The FFF implants were produced in an Arcam EBM S12 system (Arcam AB, Mölndal, Sweden) from a standard Arcam Ti6Al4V ELI powder with a particle size of between 45 and 100 μm . The electron beam melted the powder in a layer-by-layer process with a layer thickness of 0.1 mm. The average building temperature of the powder bed and the vacuum pressure inside the chamber were $\sim 550^\circ\text{C}$ and 5×10^{-4} mbar, respectively. All the implants were produced in a single build with the same process controlling the settings. After the build was completed, the implants were cooled inside the chamber in an He atmosphere (200 mbar) until the temperature within the powder bed reached 100°C . Air was then introduced into the chamber.

Cleaning

All the implants were cleaned ultrasonically with MIS 024 (Tremedic AB, Göteborg, Sweden) for 10 min, followed by ultrasonic cleaning for 15 min with ELGA/Milli-Q water (Tremedic AB, Göteborg, Sweden). The implants were then placed in sterile bags and steam autoclaved.

Material Characterization

Material Properties of Bulk Samples. The properties of the FFF material were obtained from tensile bars produced from standard Arcam Ti6Al4V ELI powder (particle size 45–100 μm and layer thickness 0.1 mm).

Surface Chemistry. The chemical surface properties of six samples noted as A/1&2, B/1&2, and C/1&2 were studied by Auger electron spectroscopy (AES) analysis.

In addition to X-ray photoemission spectroscopy, AES is a well-established method for determining the chemical composition of surfaces. The sample is irradiated by a reasonably mono-energetic electron beam, resulting in the emission of secondary so-called Auger electrons. The kinetic energies of these electrons are defined by the atoms with which they were associated before the emission. AES is a fast, sensitive method and is well suited for measuring the chemical composition, as it permits depth concentration profiles, when used in combination with ion sputtering.

For quantitative AES analysis and depth profiles, a PHI 660 scanning auger microprobe was used. Measurements for quantitative analysis were made at four points for each of the samples. The electron beam was defocused to cover a larger area, thereby lowering the radiation damage and attaining a true average surface composition. The analysis parameters are listed in Table I. The AES spectra were measured with 11-point smoothing before five point

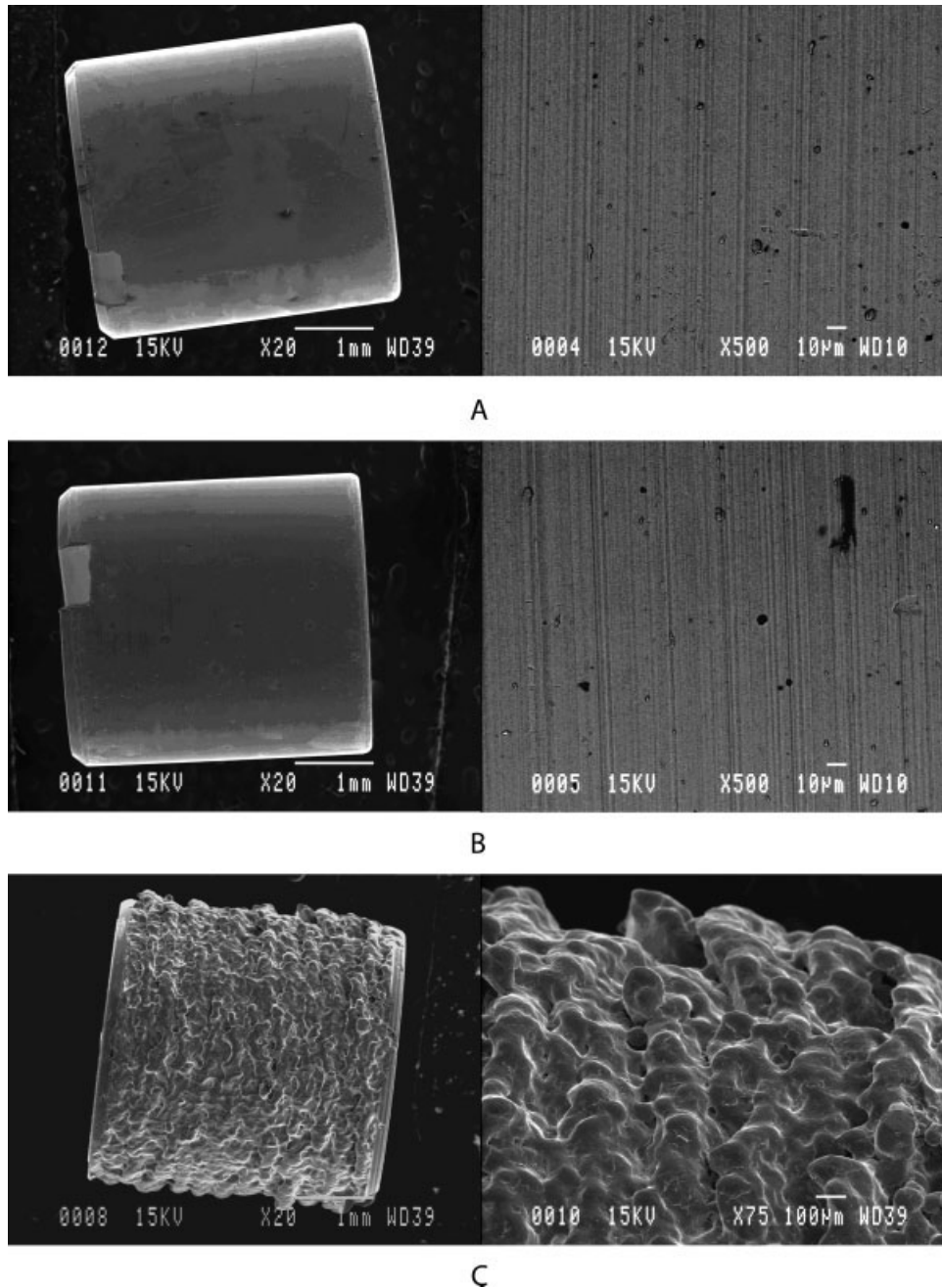


Figure 1. Survey (to the left) and high magnification (to the right) scanning electron micrographs of implants (A), (B), and (C), respectively. Typical ridges and valleys due to machining are shown for implants (A) and (B). For implant (C), a wavy surface texture with rounded protrusions and multiple crevices and invaginations is shown.

differentiation before quantification. Depth profiles were acquired from three of the samples; A/2, B/2, and C/2. A sputtering rate of 2 nm/min was used.

Surface Topography. It was not possible to determine the surface topography for the net-shaped implant C, because its curvature was too large when compared with its rough surface. Instead, a larger FFF sample (Figure 2) was used. This sample was built in the same build as the implants, and its surface topography was therefore expected

TABLE I. Analysis Parameters Used for AES

Parameter	
Primary beam energy (E_p)	3.0 keV
Beam current (I)	400 nA
Analyzed area, diameter	150 μm
Analyzer resolution	0.6%
Spectrum width	30–1080 eV
Analysis time	50 ms/eV
Number of scans at each point	5

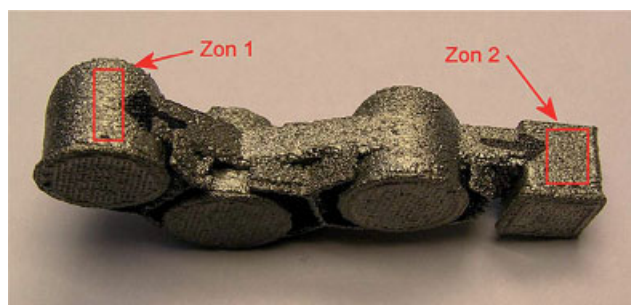


Figure 2. The larger sample used for interference profilometry of net-shaped implants. [Color figure can be viewed in the online issue, which is available at www.interscience.wiley.com.]

to be similar to that of implant C. The measurements were made with an optical interferometer (Wykon NT 2000). Implants A/2 and B/2 were studied on two surfaces using a $90 \times 120 \mu\text{m}^2$ surface measurement area. On the larger sample, two surface areas for each region (cf. Figure 2) were studied. The size of these areas was $1800 \times 2400 \mu\text{m}^2$. Because of the rough surface of the larger sample, no signals were recorded from some parts of the areas in region 1. In this case, an interpolation procedure was used to obtain data over the entire area. The following topographical parameters were determined:

Amplitude parameters

S_a , the average height of structures from a mean plane

S_q , root mean square

S_{sk} , surface skewness

Hybrid parameters

S_{dr} , surface area ratio

Surgery

According to a randomized implant insertion scheme, 48 implants (16 of each type) were placed in 12-female adult New Zealand white rabbits, weighing around 5.5 kg, and fed *ad libitum*. Implant diameter and length were 3.75 mm and 4 mm, respectively. The experiments were approved by the Local Ethics Committee, Göteborg University. Before surgery, the animals were anesthetized by intramuscular (i.m.) injections of a combination of phentanyl and fluanizon [Hypnorm[®], Janssen, Brussels, Belgium; 0.7 mg/kg body weight (b.wt.)] and intraperitoneal (i.p.) injections of diazepam (Stesolid[®], Dumex, Copenhagen, Denmark; 1.5 mg/kg b.wt.). Lidocaine (5% Xylocain[®], Astra AB, Södertälje, Sweden) was infiltrated subcutaneously (s.c.) to obtain local anesthesia. The limbs were shaved and disinfected with chlorohexidine (5 mg/mL, Pharmacia AB, Stockholm, Sweden). Operations were performed under sterile conditions. Each animal received two implants of the same type in one leg and two implants of the other type in the contralateral leg. One implant was inserted in each proximal tibial metaphysis and one implant in each medial femoral condyle, according to a random schedule. The bone was exposed separately through skin incisions and blunt dissection of the underlying tissue, including the periosteum. The holes in both the tibia and femur were made using dental implantation drills of increasing size up to a diameter of 3.75 mm under profuse irrigation with sterile saline (NaCl 9 mg/mL; ACO, Sweden). The implants were then gently press fitted. The operation site was rinsed with saline, and the tissues were sutured in separate layers with Vicryl[®] 5-0 and finally intracutaneously with Monovicryl[®] 4-0. Animals were given trimetoprim 40 mg + sulfadoxin 200 mg/mL (Borgal[®] vet, Hoechst

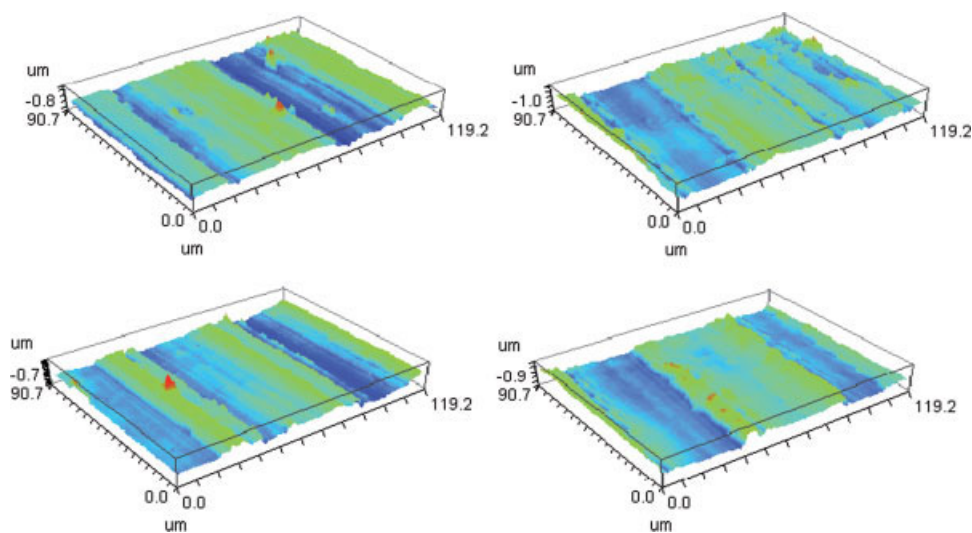


Figure 3. 3D surface topography for implant types (A) and (B). Top left A/2, area 1. Down left A/2, area 2. Top right B/2, area 1. Down right B/2, area 2. [Color figure can be viewed in the online issue, which is available at www.interscience.wiley.com.]

TABLE II. Chemical Composition of Bulk Material in Per Cent (w)

	Arcam Ti6Al4V ELI	Reference (A)	ASTM F136
Al	5.7–6.0	6.12	5.5–6.5
V	4.0	4.01	3.5–4.5
Fe	0.08–0.1	0.20	<0.25
O	0.10	0.11	<0.13
N	0.01	0.01	<0.05
H	<0.003	0.005	<0.01
C	0.03	0.02	<0.08
Ti	Balance	Balance	Balance

AB) before surgery and 2-days postoperatively. Analgesics, buprenorphine (Temgesic[®], Reckitt and Colman, 0.05 mg/mL), were given for 3-days postoperatively.

Animal Sacrifice

The animals were sacrificed after 2-weeks with an overdose of barbiturate (Mebumal[®], ACO Läkemedel AB, Solna, Sweden) and fixed by perfusion via the left heart ventricle with 2.5% glutaraldehyde in 0.05M sodium cacodylate buffer, pH 7.4. The implants and the surrounding bone were removed en bloc and further immersed in glutaraldehyde for 2–4 days. After dehydration in ethanol, the undecalcified specimens were embedded in plastic resin (LR White, the London Resin, Hampshire, UK). The specimens were divided longitudinally by sawing in the centre of the implant (Exact cutting and grinding equipment, Exact Apparatebau, Norderstedt, Germany), and ground sections (thickness: 15–20 μm) were prepared and stained with 1% toluidine blue.^{18,19}

Microscopy and Morphometry

Light microscopic morphometry was performed blind on the ground sections using a Nikon Eclipse E600 light microscope and connected to computer software. General, qualitative observations of the tissue response were made, whereas quantitative observations were made by measuring the bone-to-implant contact on each side of the cylinder. The mean values (% of direct bone contact) for all implants in each group (e.g. type A implants in the femur) were calculated and subjected to statistical comparisons. All the data are given as the mean \pm standard error of the mean.

TABLE III. Mechanical Properties of Bulk Material

	Arcam Ti6Al4V ELI	Reference (A)	ASTM F136
Yield strength (Rp 0.2)	910–940 MPa	842–874 MPa	795 MPa
Ultimate tensile strength (Rm)	950–990 MPa	1064–1095 MPa	860 MPa
Rockwell hardness	30–35 HRC	–	30–35 HRC
Elongation	14–16%	–	10%
Fatigue strength at 600 MPa	>10,000,000 cycles	–	>1,000,000 cycles
Modulus of elasticity	120 GPa	–	114 GPa

Statistics

The one-way analysis of variance with the Tukey HSD test as a multiple comparison was used for statistical comparisons.

RESULTS

Materials

Bulk Properties. The chemical composition and the mechanical properties of bulk samples are given in Tables II and III, respectively. The FFF material and the reference material used for implant A are within the specification for ASTM F136. As a result, both these materials fulfill the standard specification for wrought Ti6Al4V ELI alloy for surgical implant applications.

Surface Chemistry. The chemical composition of the implant surfaces is shown in Table IV. A similar composition was detected. One exception was the detection of a 2.1% Fe content for sample C. A possible explanation for the detection of a 2.1% Fe content for sample C could be that Fe had contaminated the FFF implants during the powder removal process that follows the EBM fabrication step.

The oxide thicknesses of the samples are summarized in Table V. Sample C displayed a markedly thicker oxide, whereas the machined samples A and B did not reveal any differences in oxide thickness.

Surface Topography. The 3D surface topographies are shown in Figures 3 and 4. In Table VI, a summary of the surface topography measurements is given. Samples A and B had similar smooth surface topographies, resulting from the machining. Sample C had increased surface roughness, as judged by measurements on the large test sample.

Biological Response

Femur. The implants were inserted in the medial condyle of the right and left femur. The implantation sites healed uneventfully. Morphological observations of ground sections enabled the examination of the general tissue response around the implants. One characteristic feature of the bone response after 6-weeks was the formation of newly regenerated bone around all three types of implant (A, B, and C) (Figure 5). The bone was lamellar and had

TABLE IV. Surface AES Analysis Results in Atomic Per Cent

Sample		Ti	O	C	P	S	Ca	Si	Cu	Na	Fe	Al
A	Mean	9.8	29.1	58.1	0.1	0.4	0.7	0.9	0.5	0.2	0.0	0.1
	Std. Dev.	5.9	14.2	21.6	0.1	0.1	0.5	0.8	–	–	–	–
B	Mean	10.9	32.9	53.4	0.0	0.8	1.2	0.4	0.0	0.0	0.0	0.4
	Std. Dev.	1.8	4.6	6.5	–	0.2	0.5	0.1	–	–	–	0.2
C	Mean	11.1	35.3	49.5	0.1	0.7	0.5	0.6	0.0	0.0	2.1	0.1
	Std. Dev.	1.1	4.9	5.8	0.0	0.2	0.2	0.3	–	–	0.5	0.1

signs of remodeling. A large part of the implant periphery was in contact with osteoid, mineralized bone, and bone marrow. There were generally few signs of inflammation. No material fragments or particles were detected in the surrounding tissue.

Tibia. The implants were inserted in the proximal metaphysis of the right and left tibia. The implantation sites healed uneventfully. Newly regenerated bone was detected around all three types of implant (A, B, and C) (Figure 6). One prominent observation around the majority of implants, irrespective of implant type, was the down-growth of endosteal bone towards the part of the implant located in the bone marrow. As detected around the femoral implants, this bone had a lamellar character with ongoing bone remodeling. Few signs of inflammation were detected. A large part of the implant periphery was in contact with osteoid, mineralized bone, and bone marrow. No material fragments or particles were detected in the surrounding tissue.

Histomorphometry. Light microscopic morphometry was performed on all the implants and was performed blind by one examiner. The quantitative data can be found in Table VII for the implants in the femur and tibia, respectively. A large part of the implant surface was in direct contact with mineralized bone. There were no statistically significant differences in bone contact between the three types of implant.

DISCUSSION

The present results reveal that the FFF Ti6Al4V implants did not show any appreciable difference in tissue response in short-term behavior when compared with the conventional wrought titanium alloy implants. The general tissue response was similar for all three implant types with no evidence of inflammatory or other adverse reactions. A

TABLE V. Oxide Thickness Obtained when then Measured Oxygen Signal Dropped to Half its Maximum Value

Sample	Oxide Thickness (nm)
A/2	6
B/2	6
C/2	25

large part of the implant surfaces was in direct contact with mineralized bone, but no statistically significant differences in bone contact were found between the three types of implant. The morphology of the tissue in contact with and adjacent to the implants showed that bone was of the mature, lamellar type with no remaining inflammation after surgery, as judged by light microscopy. No differences with respect to bone maturity were observed. This does not exclude the possibility that differences could be found on the ultra structural level. The opportunity to produce ultra-thin sections for transmission electron microscopy of the intact implant-bone interface using a focused ion beam has recently been suggested.²⁰ A technique of this kind could be suitable for further studies.

The purpose of the present study was to evaluate the bone response near the interface with the material surfaces. This analysis revealed osseointegration on the morphological level. Future studies need to correlate these observations with a biomechanical evaluation of separate implants. However, previous studies have demonstrated significant correlations between torque and the percentage of bone in contact with the implant and between pull-out load and the bone thickness around the implant.²¹

The materials in the FFF implants fulfilled the standard specification for wrought Ti6Al4V ELI alloy intended for surgical implant applications. A similar surface chemical composition was detected for all three implants, with the exception of the higher Fe content in sample C, presumably caused by the powder removal process in EBM manufacturing.

One important observation in the present study was the markedly larger oxide thickness on sample C, in comparison with the machined samples A and B, which did not

TABLE VI. Summary of Surface Topography Measurements

Sample	S_a [μm]	S_q [μm]	S_{sk}	S_{dr}
A/2 area 1	0.21	0.25	–0.25	0.02
A/2 area 2	0.17	0.21	0.40	0.02
B/2 area 1	0.18	0.22	0.78	0.04
B/2 area 2	0.18	0.22	0.51	0.03
^a C reg. 1, area 1	21.39	28.28	0.181	0.23
^a C reg. 1, area 2	22.30	30.12	0.56	0.27
^a C reg. 2, area 1	15.12	19.11	–0.15	0.15
^a C reg. 2, area 2	16.25	21.95	0.82	0.16

^a Measured on the larger reference sample.

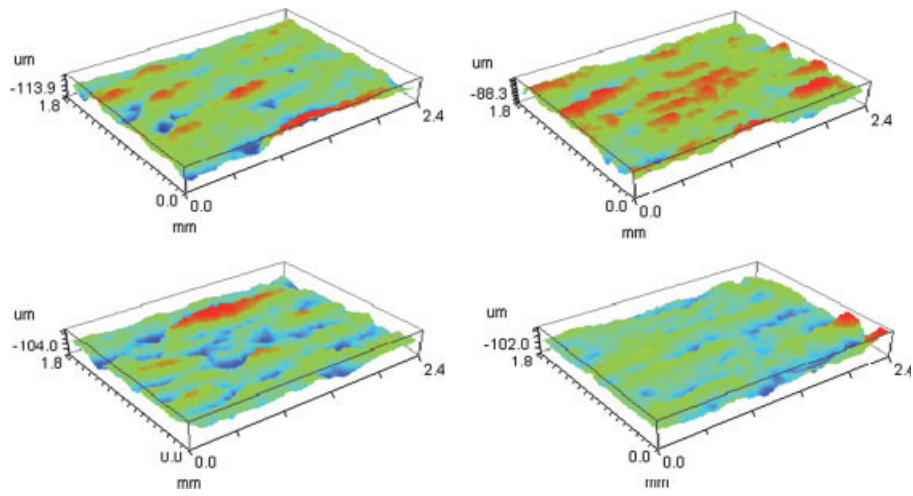


Figure 4. 3D surface topography of the large sample. Top left region 1, area 1. Down left region 1, area 2. Top right region 1, area 1. Down right region 2, area 2. [Color figure can be viewed in the online issue, which is available at www.interscience.wiley.com.]

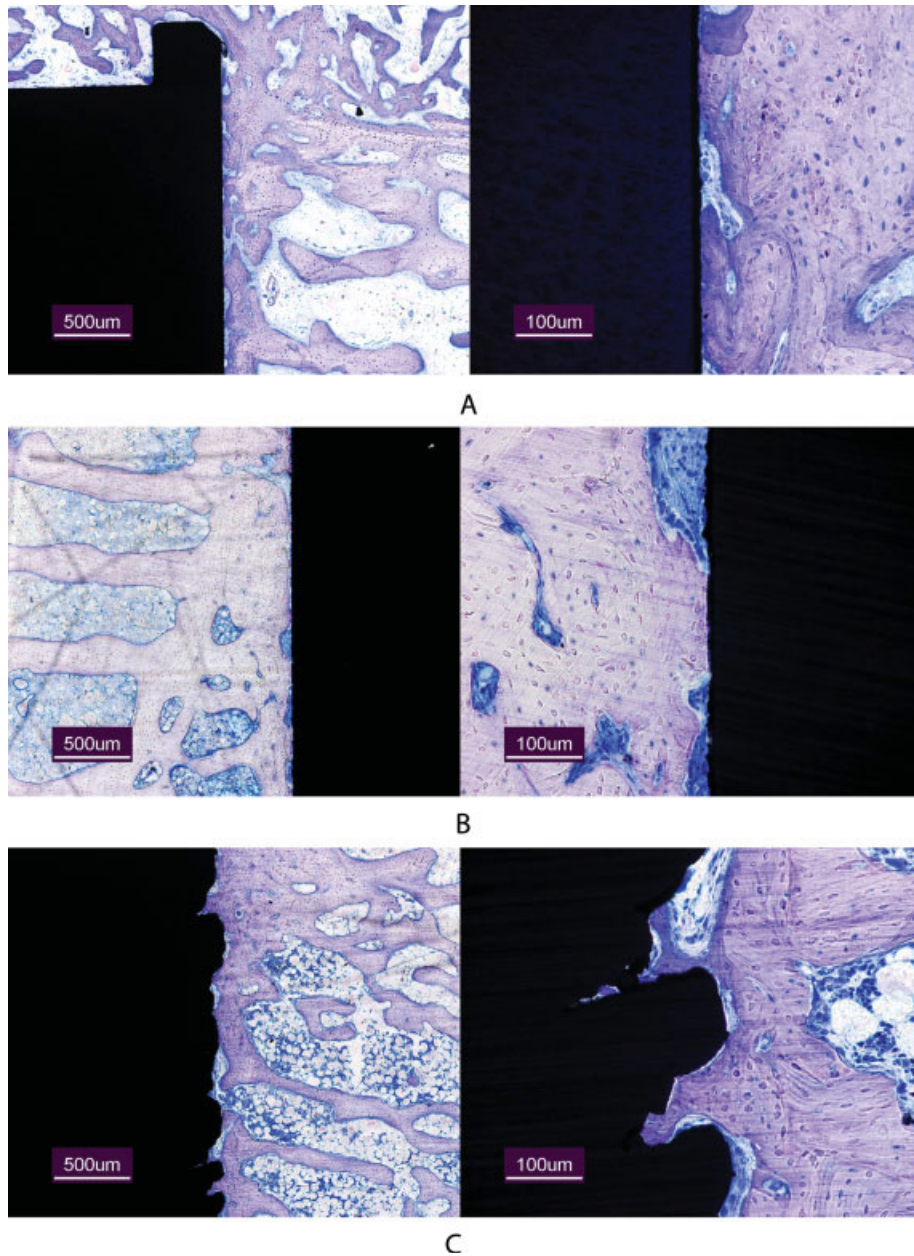


Figure 5. Survey (to the left) and high magnification (to the right) light microscopy micrographs of femur implants (A), (B), and (C), respectively. The bone is in close contact with the implants and, in the case of implant (C), the bone follows the irregularities of the implant surface. [Color figure can be viewed in the online issue, which is available at www.interscience.wiley.com.]

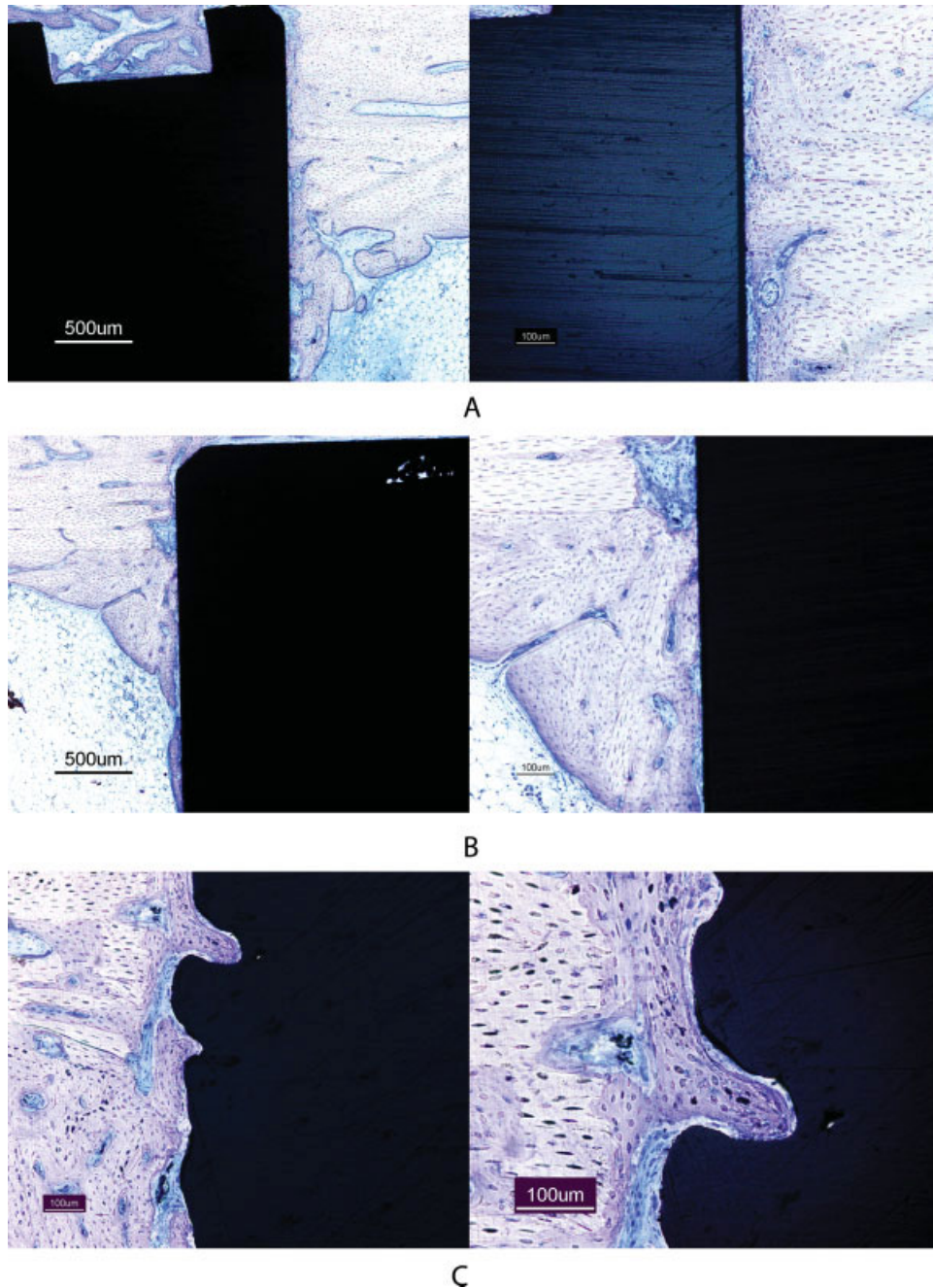


Figure 6. Survey (to the left) and high magnification (to the right) light microscopy micrographs of tibia implants (A), (B), and (C), respectively. The bone is in close contact with the implants and, in the case of implant (C), the bone follows the irregularities of the implant surface. [Color figure can be viewed in the online issue, which is available at www.interscience.wiley.com.]

reveal any differences in oxide thickness. Although the machined samples and sample C had a similar bone response, with no significant difference regarding bone contact as judged by light microscopy and histomorphometry, it is difficult exactly to determine the role of each property (i.e. oxide thickness and surface roughness) in the observed net biological results.

In vitro and *in vivo* studies have provided strong indications that the biological response to titanium is influenced by both surface structure (roughness) and chemical

TABLE VII. Histomorphometry

Implant	Bone Contact (%)	
	Femur	Tibia
A	29 ± 3	36 ± 4
B	35 ± 5	33 ± 5
C	41 ± 3	31 ± 3

Bone-implant contact (%).

There are no statistically significant differences between the materials.

Femur: A-B = $p < 0.499$, A-C = $p < 0.061$, B-C = $p < 0.464$.

Tibia: A-B = $p < 0.896$, A-C = $p < 0.689$, B-C = $p < 0.919$.

composition.^{22–32} The properties of titanium implants, such as topography and roughness, oxide thickness and microstructure, oxide composition, impurity levels, and so on, vary considerably, depending on the type of surface preparations that are used.³¹ The surface properties of titanium can be varied over a wide range in a more or less controlled and systematic manner, provided that the correct preparation and characterization procedures are used. One possible explanation for the relatively thicker oxide layer in sample C could be that, in the case of powder particles, the main oxygen content is situated on the surfaces. As the particles melt, most of the oxygen is dissolved into the material, whereas some oxygen is released into the surroundings. As a result, FFF bulk material usually has a somewhat lower content of oxygen than the original powder. However, the particles at the interface between melted metal and powder are not completely melted. As a result, these particles may have an increased oxide thickness.

In comparison with the relatively smooth samples A and B, the S_a and S_q values of sample C were ~ 100 times higher than the others. The amplitudes of the variations in the rough surfaces were therefore of the same order as the powder particle size. However, the S_{sk} values were similar for all samples, indicating that the skewness, the asymmetry of the surface deviation about the mean surface, was similar for all samples. The S_{dr} value reflects the hybrid properties of the surfaces, with a large value indicating the significance of either amplitude or spacing or both. Clearly, in the case of the rough surface, the S_a and the S_q values indicate that there are significant contributions from amplitude variations. However, it is clear that there is a wave-like spacing between the amplitudes (cf. Figure 4). The waviness is in the y -direction, which is the same direction as the layer-by-layer build process. The wavelength cannot be directly connected with the layer thickness. It is understood that both the wavelength and the amplitude are complex functions of process parameters, layer thickness, and powder particle size. This functional behavior needs to be examined thoroughly in future investigations and it is not within the scope of this study.

The present results revealed greater surface roughness and an equal percentage of bone-to-metal contact in the FFF sample C, compared with the turned surfaces. This means that the absolute contact with bone is greater for sample C. This may create a more biomechanically favorable situation. However, with an “excess” of surface roughness, the available surface area for potentially adverse effects, such as ion release, potential crevices for microorganisms, and so on, will increase. In addition, the surface roughness denotes features on scales of different length, ranging from macro- to nano-topographical features. The roughness of titanium implants modulates osteoblast attachment, proliferation, and differentiation.³³ However, macrophages which orchestrate inflammation and tissue repair prefer rough surfaces to smooth ones, exhibiting rugophilia.^{34,35}

To summarize, the present results show that EBM, FFF, experimental Ti6Al4V implants acquire increased oxide thickness and surface roughness. Short-term experimental studies in bone reveal a similar biological response in cortical and trabecular bone for native FFF implants of this type in comparison with machined and conventionally wrought material. It is concluded that, provided careful control of the mechanical and surface properties is made, CAD and FFF technologies offer the potential to customize and produce implants with new, hitherto unmatched properties, such as complex shape, size, and interconnectivity, which justify further long-term studies in animals and subsequent human implantation.

Arcam AB is a partner of the BIOMATCELL VINN Excellence Center of Biomaterials and Cell Therapy, hosted by the Sahlgrenska Academy at University of Gothenburg.

REFERENCES

1. Brånemark R, Brånemark P-I, Rydevik R, Myers RR. Osseointegration in skeletal reconstruction and rehabilitation: a review. *J Rehabil Res Dev* 2001;38:175–181.
2. Henry PJ. Clinical experiences with dental implants. *Adv Dent Res* 1999;13:147–152.
3. Hallman M, Mordenfeld A, Strandkvist T. A retrospective 5-year follow-up study of two different titanium implant surfaces used after interpositional bone grafting for reconstruction of the atrophic edentulous maxilla. *Clin Implant Dent Relat Res* 2005;7:121–126.
4. Laine P, Salo A, Kontio R, Ylijoki S, Lindqvist C, Suuronen R. Failed dental implants—Clinical, radiological and bacteriological findings in 17 patients. *J Craniomaxillofac Surg* 2005;33:212–217.
5. Thor A, Wannfors K, Sennerby L, Rasmusson L. Reconstruction of the severely resorbed maxilla with autogenous bone, platelet-rich plasma, and implants: 1-year results of a controlled prospective 5-year study. *Clin Implant Dent Relat Res* 2005;7:209–220.
6. Buser D, Martin W, Belser UC. Optimizing esthetics for implant restorations in the anterior maxilla: Anatomic and surgical considerations. *Int J Oral Maxillofac Implants* 2004;19 (Suppl):43–61.
7. Harvey BV. Optimizing the esthetic potential of implant restorations through the use of immediate implants with immediate provisionals. *J Periodontol* 2007;78:770–776.
8. Nag S, Banerjee R, Fraser HL. A novel combinatorial approach for understanding microstructural evolution and its relationship to mechanical properties in metallic biomaterials. *Acta Biomater* 2007;3:369–376.
9. Ostman PO, Hellman M, Sennerby L. Direct implant loading in the edentulous maxilla using a bone density-adapted surgical protocol and primary implant stability criteria for inclusion. *Clin Implant Dent Relat Res* 2005;7 (Suppl 1):S60–S69.
10. Touati B, Rompen E, Van Dooren E. A new concept for optimizing soft tissue integration. *Pract Proced Aesthet Dent* 2005;17:711–712, 714–715.
11. Malmstrom J, Adolfsson E, Arvidsson A, Thomsen P. Bone response inside free-form fabricated macroporous hydroxyapatite scaffolds with and without an open microporosity. *Clin Implant Dent Relat Res* 2007;9:79–88.
12. Malmström J, Adolfsson E, Emanuelsson L, Thomsen P. Bone ingrowth in zirconia and hydroxyapatite scaffolds with

- identical macroporosity. *J Mater Sci Mater Med* 2008;19:2983–2992.
13. Lee SH, Shin H. Matrices and scaffolds for delivery of bioactive molecules in bone and cartilage tissue engineering. *Adv Drug Deliv Rev* 2007;59:339–359.
 14. Malmstrom J. On Bone Regeneration in Porous Bioceramics—Studies in Humans and Rabbits Using Free Form Fabricated Scaffolds. Göteborg: University of Göteborg, Sweden; 2007.
 15. Larsson. Patent, SE 9301647, 1993.
 16. Larsson C. The Interface Between Bone and Metals with Different Surface Properties—Light Microscopic and Ultrastructural Studies. Gothenburg: Göteborg University; 1997.
 17. Larsson M, Lindhe U, Harrysson O. Rapid manufacturing with electron beam melting (EBM)—A manufacturing revolution? In: Bourell D, et al, editors. *Proceedings Solid freeform fabrication symposium*. Austin, TX; 2003. pp 433–438.
 18. Donath K. Die Trenn-Dunnschliff-Technik zur Herstellung histologischer Präparaten von nicht schneidbaren Geweben und Materialien. *Der Präparator* 1988;34:318–325.
 19. Donath K, Breuner G. A method for the study of undecalcified bones and teeth with attached soft tissues. The Sage-Schliff (sawing and grinding) technique. *J Oral Pathol* 1982;11:318–326.
 20. Engqvist H, Botton GA, Couillard M, Mohammadi S, Malmström J, Emanuelsson L, Hermansson L, Phaneuf MW, Thomsen P. A novel tool for high-resolution transmission electron microscopy of intact interfaces between bone and metallic implants. *J Biomed Mater Res A* 2006;78:20–24.
 21. Brånemark R, Öhrnell L-O, Nilsson P, Thomsen P. Biomechanical characterization of osseointegration during healing: An experimental in vivo study in the rat. *Biomaterials* 1997;18:969–978.
 22. Cooley DR, Van Dellen AF, Burgess JO, Windeler AS. The advantages of coated titanium implants prepared by radiofrequency sputtering from hydroxyapatite. *J Prosthet Dent* 1992;67:93–100.
 23. Hazan R, Brener R, Oron U. Bone growth to metal implants is regulated by their surface chemical properties. *Biomaterials* 1993;14:570–574.
 24. Swart KM, Keller JC, Wightman JP, Draughn RA, Stanford CM, Michaels CM. Short-term plasma-cleaning treatments enhance in vitro osteoblast attachment to titanium. *J Oral Implantol* 1992;18:130–137.
 25. Chehroudi B, Gould TR, Brunette DM. Effects of a grooved titanium-coated implant surface on epithelial cell behavior in vitro and in vivo. *J Biomed Mater Res* 1989;23:1067–1085.
 26. Chehroudi B, Gould TR, Brunette DM. Titanium-coated micromachined grooves of different dimensions affect epithelial and connective-tissue cells differently in vivo. *J Biomed Mater Res* 1990;24:1203–1219.
 27. Therin M, Meunier A, Christel P. A histomorphometric comparison of the muscular tissue reaction to stainless steel, pure titanium and titanium alloy implant materials. *J Mater Sci Mater Med* 1991;2:1–8.
 28. Ricci JL, Spivak JM, Blumenthal N, Alexander H. *Modulation of Bone Ingrowth by Surface Chemistry and Roughness*. Toronto: Toronto University Press; 1991.
 29. Buser D, Schenk RK, Steinemann S, Fiorellini JP, Fox CH, Stich H. Influence of surface characteristics on bone integration of titanium implants. A histomorphometric study in miniature pigs. *J Biomed Mater Res* 1991;25:889–902.
 30. Könönen M, Hormia M, Kivilahti J, Hautaniemi J, Thesleff I. Effect of surface processing on the attachment, orientation, and proliferation of human gingival fibroblasts on titanium. *J Biomed Mater Res* 1992;26:1325–1341.
 31. Lausmaa J. Surface spectroscopic characterization of titanium implant materials. *J Electron Spectr Related Phenom* 1996;81:343–361.
 32. Larsson C, Emanuelsson L, Thomsen P, Ericson LE, Aronsson BO, Kasemo B, Lausmaa J. Bone response to surface modified titanium implants—Studies on the tissue response after 1 year to machined and electropolished implants with different oxide thicknesses. *J Mater Sci Mater Med* 1997;8:721–729.
 33. Boyan BD, Dean DD, Lohmann CH, Cochran DL, Sylvia VL, Schwartz Z. The titanium-bone cell interface in vitro: The role of the surface in promoting osteointegration. In: Brunette DM, Tengvall P, Textor M, Thomsen P, editors. *Titanium in Medicine*. Berlin: Springer; 2001, Ch. 17, pp 562–585.
 34. Rich A, Harris AK. Anomalous preferences of culture macrophages for hydrophobic and roughened substrata. *J Cell Sci* 1981;50:1–7.
 35. Brunette DM. Principles of cell behavior on titanium surfaces and their applications to implanted devices. In: Brunette DM, Tengvall P, Textor M, Thomsen P, editors. *Titanium in Medicine*. Berlin: Springer; 2001, Ch. 15, pp 486–512.